

Transmission of information and synchronization in a pair of coupled chaotic circuits: an experimental overview

M. S. Baptista^{1 a}, S. P. Garcia^{1 b}, S. K. Dana^{2 c}, and J. Kurths^{3 d}

¹ Max-Planck-Institute für Physik komplexer Systeme, Nöthnitzer Str. 38, D-01187 Dresden, Deutschland

² Central Instrumentation, Indian Institute of Chemical Biology (Council of Scientific and Industrial Research), Kolkata 700032, India

³ Potsdam Institute for Climate Impact Research, Telegraphenberg, Potsdam, Germany

Abstract. We propose a rationale for experimentally studying the intricate relationship between the rate of information transmission and synchronization level in active networks, applying theoretical results recently proposed. We consider two non-identical coupled Chua's circuit with non-identical coupling strengths in order to illustrate the proceeding for experimental scenarios of very few data points coming from highly non-coherent coupled systems, such that phase synchronization can only be detected by methods that do not rely explicitly on the calculation of the phase. A relevant finding is to show that for the coupled Chua's circuit, the larger the level of synchronization the larger the rate of information exchanged between both circuits. We further validate our findings with data from numerical simulations, and discuss an extension to arbitrarily large active networks.

1 Introduction

Given an arbitrary time dependent stimulus that externally excites an active network, formed by elements that have some intrinsic dynamics (e.g. neurons or oscillators), how much information from such stimulus can be realized by measuring the time evolution of one of the elements of the network? For example, in neurosciences, determining how and how much information flows along anatomical brain paths is an important requirement for understanding how animals perceive their environment, learn and behave [1,2,3].

Even though the approaches in Refs. [1,2,3,4,5,6] have brought considerable understanding on how and how much information from a stimulus is transmitted in a neural network, the relationship between synchronization and information transmission in a neural as well as in an active network is still awaiting a more quantitative description.

In order to treat this problem in a more analytical way, we proceed in the same line as in Refs. [7,8], and study the information transfer in autonomous networks. However, instead of treating the information transfer between dynamical systems components, we treat the transfer of information per unit time exchanged between two elements in an autonomous chaotic active

^a Corresponding author: baptista.murilo@gmail.com

^b spinto@pks.mpg.de; Present address: Signal Processing Laboratory, IEETA, University of Aveiro, Campus Universitário de Santiago, 3810-193 Aveiro, Portugal.

^c skdana@iicb.res.in

^d juergen.kurths@pik-potsdam.de

network [9]. Arguably, the relationship between synchronization and information in autonomous chaotic networks is useful for understanding its counterpart in non-autonomous active networks.

The purpose of the present work is to revisit some previous theoretical results and explain how to apply such approaches to study information transmission and synchronization from data coming from experiments.

In Refs. [9], we proposed a formula [see Eq. (10)] that enables the calculation of the rate with which information is exchanged between two elements in a chaotic network, in terms of defined positive conditional Lyapunov exponents. Consider two non-identical coupled chaotic systems with two positive conditional exponents, λ^{\parallel} and λ^{\perp} . The upper bound for the rate with which information is exchanged between these two elements is given by $\lambda^{\parallel} - \lambda^{\perp}$.

While Lyapunov exponents measure the exponential divergence of nearby trajectories in phase space, the conditional Lyapunov exponents measure the exponential divergence of nearby trajectories on a coordinate-transformed space. This transformed space (see Sec. 4) is constructed in such a way that if the elements in a network are almost completely synchronous [10, 11, 12], then one conditional exponent, λ^{\parallel} , measures the exponential divergence of trajectories along the synchronization manifold, and the other exponent, λ^{\perp} , measures the exponential divergence of trajectories along the transversal manifold. Then, the rate of information exchanged between two elements is the rate of information produced by the synchronous trajectories (λ^{\parallel}) minus the rate of information produced by the desynchronous trajectories (λ^{\perp}). Thus, this formula enables one to understand the relationship between information and synchronization, since the so defined conditional exponents are a measure of the synchronization and desynchronization between two elements in a network.

We apply the formula proposed in Refs. [9] using an experimental perspective. We consider that one has only a short time series available to do the analysis and that the system is highly non-coherent. Under such conditions, we will show that the largest Lyapunov exponent of a two coupled Chua's circuit [13] can only be well estimated using a bivariate time series that contains information of the trajectories of both circuits. Further, we show that the second largest Lyapunov exponent can only be roughly estimated by using information from the characteristic of conditional observations performed in one circuit while the other realizes some event. These conditional observations, defined in Refs. [14, 15], are in fact an alternative way of detecting phase synchronization [16, 17] without having to actually measure the phase. Such a method is a necessary tool in order to study phase synchronization in non-coherent systems whose phases might not always be well defined, as the one considered here, the two non-identical diffusively coupled Chua's oscillators, with non-identical coupling strengths (Sec. 2).

We start by showing how one can measure phase synchronization in this coupled circuit (Sec. 3). Further, we demonstrate (Sec. 4) that Eq. (10) can be written in terms of the positive Lyapunov exponents, thus enabling the use of standard codes to study information transmission in coupled chaotic systems. Since the amount of data points in each time series is small, alternative techniques to calculate the second largest Lyapunov exponent will be developed (Sec. 4.1). The direct relationship between synchronization and information, one of the main results of this work, is detailed in Sec. 5, and finally, in Sec. 6, we discuss how to extend our results to larger networks with arbitrary connecting topologies.

2 Experimental and numerical simulation setups

2.1 Experiment

We consider two diffusively coupled non-identical Chua's circuits [13] as shown in Fig. 1. Each oscillator is composed by a resistor $R_{1,8}$, an inductor $L_{1,2}$, two capacitors $C_{1,3}$ and $C_{2,4}$, and one piecewise-linear resistance. In our notation, the first (second) index denotes an element in the upper (lower) circuit of Fig. 1. The upper circuit is regarded as S_1 and the lower as S_2 . The piecewise-linear resistance is designed by a pair of linear amplifiers, U_1 - U_2 (in S_1) or U_3 - U_4 (in S_2) with an op-amp 741 μ A, for each oscillator. The resistance R_C sets the coupling strengths, $\epsilon_1 = \frac{R_1}{R_C}$ and $\epsilon_2 = \frac{R_8}{R_C}$.

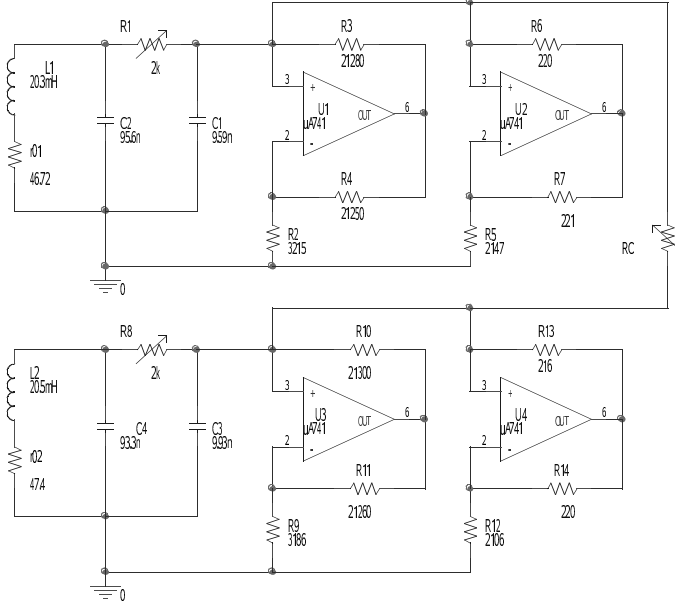


Fig. 1. Two diffusively coupled Chua's oscillators with a power supply of $\pm 9V$, and parameters $L_1=20.5mH$, $r_{01}=47.46\Omega$, $C_1=9.56nF$, $C_2=95.9nF$, $R_2=3215\Omega$, $R_3=21.28k\Omega$, $R_5=2147\Omega$, $L_2=20.3mH$, $r_{02}=46.98\Omega$, $C_3=9.93nF$, $C_4=93.3nF$, $R_9=3186\Omega$, $R_{10}=21.26k\Omega$, $R_{12}=2106\Omega$.

Two state variables, $x_1 = V_{C1}$ and $x_2 = V_{C3}$, are monitored using two channels of a digital oscilloscope (Tektronix, TDS 220) at the nodes of the capacitors C_1 and C_3 , respectively, for varying coupling resistance R_C . Data acquisition is made for 2500 data points at each snapshot by an 8-bit memory of the oscilloscope, with a time step-size $\Delta t=0.002ms$. All circuit component values are precisely measured using a standard LCR-Q bridge (APLAB 4910). We consider 20 data sets denoted by F_o , with $o = \{1, \dots, 20\}$ representing the value of R_C . The larger o is, the larger R_C is. The set denoted as F_{21} contains data from the uncoupled circuits ($\epsilon=0$).

2.2 Simulation

To simulate the equations of motion of the circuit in Fig. 1, we use the dimensionless set of equations given by

$$\begin{aligned} \frac{dx_i}{d\tau} &= \tau_i \alpha_i [y_i - x_i - f(x_i)] + \epsilon_i \tau_i \alpha_i (x_j - x_i) \\ \frac{dy_i}{d\tau} &= \tau_i (x_i - y_i + z_i) \\ \frac{dz_i}{d\tau} &= \tau_i (-\beta_i y_i - \gamma_i z_i) \end{aligned} \quad (1)$$

where $(i, j) = (1, 2)$ with $j \neq i$, $\tau_1=1$, $\tau_2 = \frac{R_1 C_2}{R_8 C_4}$, $\alpha_1 = \frac{C_2}{C_1}$, $\beta_1 = \frac{R_1^2 C_2}{L_1}$, $\gamma_1 = \frac{R_1 r_{01} C_2}{L_1}$, $\alpha_2 = \frac{C_4}{C_3}$, $\beta_2 = \frac{R_8^2 C_4}{L_2}$, $\gamma_2 = \frac{R_8 r_{02} C_4}{L_2}$, $\epsilon_1 = \frac{R_1}{R_C}$, and $\epsilon_2 = \frac{R_8}{R_C}$. The state variables are the dimensionless voltages $x_1 = \frac{V_{C1}}{E}$, $x_2 = \frac{V_{C3}}{E}$, $y_1 = \frac{V_{C2}}{E}$, $y_2 = \frac{V_{C4}}{E}$ (at the respective capacitor nodes), $z_1 = \frac{R_1 I_{L1}}{E}$, and $z_2 = \frac{R_8 I_{L2}}{E}$ (where $I_{L1, L2}$ is the inductor current). E is the saturation voltage of the op-amps approximated as $E \approx 1$.

The parameters considered for the numerical simulations are $r_{01}=47.46$, $r_{02}=46.98$, $R_1=1650$, $R_2=3224$, $R_3=21300$, $R_4=21330$, $R_5=2153$, $R_6=221.6$, $R_7=220.6$, $R_8=1650$, $R_9=3194$, $R_{10}=21320$, $R_{11}=21330$, $R_{12}=2111$, $C_1=9.56 \times 10^{-9}$, $C_2=95.9 \times 10^{-9}$, $C_3=9.93 \times 10^{-9}$, $C_4=93.3 \times 10^{-9}$, $L_1=20.5$

$\times 10^{-3}$ and $L_2=20.3 \times 10^{-3}$. Components have standard units as Ohm for resistance, Farad for capacitance and Henry for inductance.

The piecewise-linear function $f(x_{1,2})$ is defined as

$$f(x_{1,2}) = \begin{cases} b_{1,2}x_{1,2} + (b_{1,2} - a_{1,2}), & \text{if } x_{1,2} < -1 & \rightarrow \text{Domain } D_- \\ a_{1,2}x_{1,2}, & \text{if } -1 \leq x_{1,2} \leq 1 & \rightarrow \text{Domain } D_0 \\ b_{1,2}x_{1,2} + (a_{1,2} - b_{1,2}), & \text{if } x_{1,2} > 1 & \rightarrow \text{Domain } D_+ \end{cases} \quad (2)$$

where $a_{1,2} = (-\frac{1}{R_{2,9}} - \frac{1}{R_{5,12}})R_{1,8}$ and $b_{1,2} = (\frac{1}{R_{3,10}} - \frac{1}{R_{5,12}})R_{1,8}$. The piecewise linear function $f(x_{1,2})$ has a slope $a_{1,2}$ in the inner region near the equilibrium at the origin (domain D_0) and a slope $b_{1,2}$ in the outer regions close to the two mirror symmetric equilibria of each oscillator (domains D_+ and D_-).

The dimensionless variables in the time- τ frame of the numerical simulations are obtained by rescaling the time- t frame of the experiment by $\tau = \frac{t}{R_1 C_2}$.

3 Phase, phase synchronization, and conditional maps

Phase synchronization (PS) [16] is a phenomenon defined by

$$|\Delta\phi(S_1, S_2)| = |\phi_1 - m\phi_2| \leq r, \quad (3)$$

where ϕ_1 and ϕ_2 are the phases of two elements S_1 and S_2 , $m = \omega_2/\omega_1$ is the angular frequency ratio that can be a real number [17], and ω_1 and ω_2 are the average frequencies of oscillation of the elements S_1 and S_2 . The phase ϕ is a function constructed on a 2D subspace, whose trajectory projection has proper rotation, i.e. it rotates around a well defined center of rotation. The Chua's circuit, while presenting a double scroll attractor, has no proper rotation in the phase space, but it can have proper rotation in the velocity space, therefore it can admit a phase that measures the displacement of the tangent vector [14,18] and can be calculated as shown in Ref. [18] by

$$\phi(t) = \int_0^t \frac{\ddot{y}\dot{x} - \ddot{x}\dot{y}}{(\dot{x}^2 + \dot{y}^2)} dt. \quad (4)$$

However, as neither the simulated nor the experimental circuit, for $\epsilon \neq 0$, present proper rotation in both phase and velocity spaces, Eq. (4) has only physical meaning for a time interval where the attractors are far away from the equilibrium points, a time that can be large but not infinitely large. Therefore, for the present study is necessary to employ alternative methods that detect phase synchronization without having to measure the phase, as the one proposed in Refs. [14,15]. If PS exists between two subspaces, then by observing the trajectory of one circuit at the time the other circuit makes a physical event (an event that has positive probability of occurrence), there exists at least one special curve, Γ , in this subspace, for which the points obtained from these conditional observations do not visit its neighborhood. Such a curve Γ is defined in the following way. Given a point x_0 in the attractor projected onto the subspace of one circuit where the phase is defined, Γ is the union of all points for which the phase, calculated from this initial point x_0 , reaches $n\langle r \rangle$, with $n = 1, 2, 3, \dots, \infty$ and $\langle r \rangle$ a constant (typically 2π). Clearly, an infinite number of curves Γ can be defined.

For coupled systems with sufficiently close parameters that have proper rotation in some subspace, if the points obtained from the conditional observations do not visit the whole attractor projection on this subspace, one can always find a curve Γ that is far away from the conditional observations. Therefore, for such cases, to state the existence of PS one just has to check if the conditional observations are localized with respect to the attractor projection on the subspace where the phase is calculated. Note that the value of the angular frequency ratio, m , is irrelevant to state PS using these conditional mappings. Whatever m is, if there is PS, these mappings will be localized.

In a general situation, where the attractor has no proper rotation either in phase or velocity spaces and the event is a physical event, thus, as demonstrated in Ref. [15], PS implies the localization of the conditional sets.

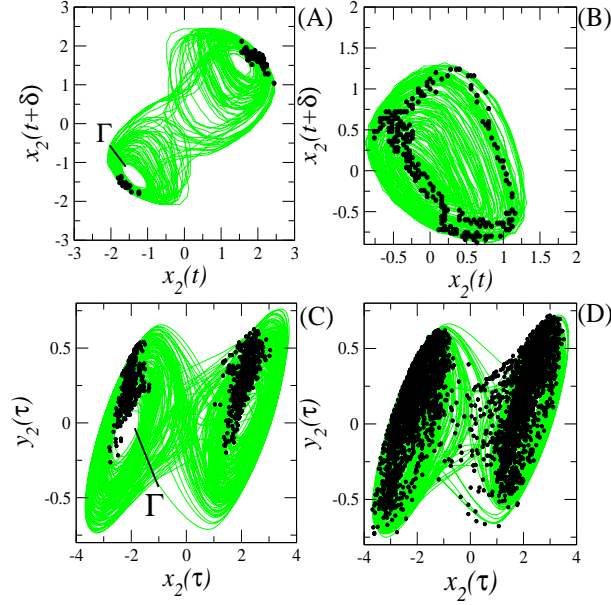


Fig. 2. [Color online] Projections of the attractor [gray (green) lines] and conditional mappings [black filled circles]. Experimental results are shown in (A-B) and simulations in (C-D). PS happens for the data set F12 (A) and it is absent for the data set F18 (B). PS is observed for $R_C=12,000$ (C) and is absent for $R_C=25,000$ (D). The conditional mappings for (A) [resp. (B)] are constructed by observing the circuit S_2 at the moment the events defined in conditions (5) and (6) [resp. Eq. (7)] happen in S_1 , and the conditional mappings in (C-D) are constructed by observing the circuit S_2 at the moment the events defined in conditions (8) and (9) happen in S_1 . The straight black line (A,C) illustrates a surface Γ .

3.1 Events

An event is considered to be the crossing of the trajectory to a Poincaré section.

The experimental Poincaré sections are defined in the 2D time-delay space, constructed using the coordinates $(x(t), x(t) + \delta)$, with the time-delay $\delta = 6\Delta\tau$, and they are given by

$$x(t + \delta) = x_c \text{ and } x(t) \geq x_c \quad (5)$$

$$x(t + \delta) = -x_c \text{ and } x(t) \leq -x_c \quad (6)$$

with $x_c=1.5$, for the data sets F1 to F16 plus F21, and

$$x(t + \delta) = x_c \text{ if } x(t) \geq x_c \quad (7)$$

with $x_c=0$, for the data sets F17 to F20. The theoretical Poincaré sections are defined as

$$x_1(t) = x_c \text{ and } y_1(t) < 0 \quad (8)$$

$$x_1(t) = -x_c \text{ and } y_1(t) < 0 \quad (9)$$

with $x_c = 2$.

3.2 Observing phase synchronization in the coupled Chua's circuit without measuring the phase

In Figs. 2(A,C), we show the presence of PS in the experiment and in the simulations, respectively, while in Figs. 2(B,D), we show the absence of such a phenomenon. While in Figs. (A,C), a surface Γ can be defined such that the conditional observations do not visit it, i.e. the conditional observations are localized with respect to the attractor, in (B,D) the conditional observations spread all over the attractor, i.e. they are not localized.

4 Mutual information rate, Lyapunov and conditional exponents

In recent publications [9], we have shown that the mutual information rate (MIR) between two elements in an active chaotic network, quantifying the amount of information per unit time that can be realized in one element, i , by measuring another element, j , is given by the sum of the conditional Lyapunov exponents associated with a parallel coordinate transformation minus the positive conditional Lyapunov exponents associated with a transversal coordinate transformation.

Assuming that every element possesses only one positive Lyapunov exponent, for every pair of elements, whose state variables are given by \mathbf{x}_i and \mathbf{x}_j , we can define a coordinate transformation $\mathbf{x}_{ij}^{\parallel} = \mathbf{x}_i + \mathbf{x}_j$ and $\mathbf{x}_{ij}^{\perp} = \mathbf{x}_i - \mathbf{x}_j$ that produces two positive conditional exponents, λ^{\parallel} and λ^{\perp} (in units of bits/unit time). The mutual information rate (MIR), denoted by $I_C(t)$, between the element \mathbf{x}_i and \mathbf{x}_j is bounded from above by $\lambda^{\parallel} - \lambda^{\perp}$, and thus

$$I_C(\mathbf{x}_i, \mathbf{x}_j) \leq \lambda^{\parallel} - \lambda^{\perp} \quad (10)$$

where equality certainly holds if the elements are identical and are either in complete synchrony or decoupled ($\epsilon = 0$).

As shown in Ref. [9], if there are $N=2$ linearly coupled chaotic systems that produce at most two positive Lyapunov exponents, λ^1 and λ^2 , with $\lambda^1 > \lambda^2$, then $\lambda^{\parallel} = \lambda^1$ and $\lambda^{\perp} = \lambda^2$, since the parallel and the transversal coordinate transformations are only rotations which do not alter the value of the Lyapunov exponents.

This result can be easily demonstrated for the system considered here, due to its linear form. Thus, we can write

$$I_C(\mathbf{x}_i, \mathbf{x}_j) \leq \lambda^1 - \lambda^2 \quad (11)$$

Making the notation $\mathbf{x} = (\mathbf{x}_1^T, \mathbf{x}_2^T)$ and $\mathbf{X} = (\mathbf{x}_{12}^{\perp T}, \mathbf{x}_{12}^{\parallel T})$, we have that

$$\dot{\mathbf{x}} = \mathbf{M}_1 \mathbf{x} + c_1 \quad (12)$$

$$\dot{\mathbf{X}} = \mathbf{M}_2 \mathbf{X} + c_2 \quad (13)$$

$$\mathbf{X} = \mathbf{M} \mathbf{x} \quad (14)$$

where \mathbf{M}_1 , \mathbf{M}_2 , and \mathbf{M} are 6×6 matrices and c_1 and c_2 are constant terms from the piecewise-linear function. Matrices \mathbf{M}_2 and \mathbf{M} are explicitly written in Appendix (Sec. 8), while matrix \mathbf{M}_1 is the Jacobian of Eqs. (1).

Writing Eqs. (12), (13), and (14) in the variational form, and making a Taylor expansion (which eliminates the constant terms), the following equations are retrieved

$$\dot{\xi} \mathbf{x} = \mathbf{M}_1 \xi \mathbf{x}, \quad (15)$$

$$\xi \dot{\mathbf{X}} = \mathbf{M}_2 \xi \mathbf{X}. \quad (16)$$

While the Lyapunov exponents of Eqs. (1) are calculated from Eq. (15), the conditional exponents are calculated from Eq. (16), both using the approach in Ref. [23]. But,

$$\xi \dot{\mathbf{x}} = \mathbf{M}^{-1} \cdot \mathbf{M}_2 \cdot \mathbf{M} \xi \mathbf{x}. \quad (17)$$

Noting that $\mathbf{M}^{-1} \cdot \mathbf{M}_2 \cdot \mathbf{M}$ is just a rotation applied to matrix \mathbf{M}_2 , and since a rotation does not change the eigenvalues of \mathbf{M}_2 , thus, the Lyapunov exponents should be equal to the conditional exponents.

Assuming that we have a large active network, the theoretical approaches proposed in [9] remain valid whenever the coordinate transformation $\mathbf{x}_{ij}^{\parallel} = \mathbf{x}_i + \mathbf{x}_j$ and $\mathbf{x}_{ij}^{\perp} = \mathbf{x}_i - \mathbf{x}_j$ successfully separate the two systems i and j from the whole network. Such a situation arises, for example, in networks of chaotic maps of the unit interval connected by a diffusive (also known as electrical or linear) all-to-all topology, where every element is connected to all other elements. These approaches were also shown to be approximately valid for chaotic networks of

oscillators connected by a diffusively all-to-all topology. The discussion on how to extend such approaches to arbitrary network topologies is given in Sec. 6.

In order to compare our results with known quantities, we will also calculate the MIR using Shannon's formalism [22]. The MIR between the two circuits can be roughly estimated by symbolizing their trajectories and then measuring the mutual information from the Shannon entropy of the symbolic sequences. The mutual information between S_1 and S_2 is given by

$$I'_S = H(S_1) - H(S_2|S_1), \quad (18)$$

where $H(S_1)$ is the uncertainty about what S_1 has sent (entropy of the message), and $H(S_2|S_1)$ is the uncertainty of what was sent, after observing S_2 . In order to estimate the mutual information between the two chaotic Chua's circuit by symbolic ways, we have to proceed with a non-trivial technique to encode the trajectory, which constitutes a disadvantage of such technique to chaotic systems. We represent the time at which the n -th event happens in S_k ($k=\{1,2\}$) by T_k^n , and the time interval between the n -th and the $(n+1)$ -th event, by δT_k^n .

We encode the events using the following rule. The i -th symbol of the encoding is a "1" if an event is found in the time interval $[i\Delta, (i+1)\Delta[$ and "0" otherwise. We choose $\Delta \in [\min(\delta T_k^n), \max(\delta T_k^n)]$ in order to maximize I'_S . Each circuit produces a symbolic sequence that is split into small non-overlapping sequences of length $l=12$. The Shannon entropy of the encoding symbolic sequence (in units of bits) is estimated by $H = -\sum_p P_p \log_2 P_p$ where P_p is the probability of finding one of the 2^l possible symbolic sequences of length l . The term $H(S_2|S_1)$ is calculated by $H(S_2|S_1) = -H(S_2) + H(S_1; S_2)$, with $H(S_1; S_2)$ representing the joint entropy between both symbolic sequences for S_1 and S_2 .

Finally, the MIR (in units of bits/unit time), denoted by I_S , is calculated from

$$I_S = \frac{I'_S}{\Delta \times l}. \quad (19)$$

The calculation of I_S by means of Eq. (19) should be expected to underestimate the real value of the MIR. Since the Chua's circuit has two time-scales, a large sequence of sequential zeros in the encoding symbolic sequence should be expected to be found between two events (large δT_k^n values), leading to a reduction in the value of $H(S_1)$, followed by an increase in the value of $H(S_2|S_1)$, as there will be a large sequence of zeros happening simultaneously in the encoding sequence for the time intervals between two events of S_1 and S_2 .

4.1 Experimental exponents

The estimation of the Lyapunov exponents from the experimental time series data was done using a method recently proposed (Ref. [19]). The first step in the algorithm is the phase reconstruction, accomplished by means of the nearest neighbor embedding with different time delays method proposed in Refs. [20]. This method considers different time delays for every embedding coordinate. The embedding dimension is estimated using the false nearest neighbors criterion proposed in Ref. [21]. The second step of this algorithm pertains estimating local tangent maps by a least-squares minimization with a pseudo-inverse method. Finally, in the third step of this method, the exponents are derived from the usual QR decomposition with a modified Gram-Schmidt method.

Due to the small number of data points and the additional fact that the coupled Chua's circuit has a highly non-coherent dynamics, a better estimate of the largest Lyapunov exponents was achieved by an attractor reconstructed from the bivariate data set $(x_1(t), x_2(t))$.

However, even the bivariate data set is not capable of providing a second largest positive Lyapunov exponent, λ^2 , which should be positive if there is not complete synchronization. So, in order to estimate λ^2 from the experimental data sets, we assume that

$$\lambda^2 = \lambda^1 \left(\frac{\max(x_2^n) - \min(x_2^n)}{\max(x_2) - \min(x_2)} \right), \quad (20)$$

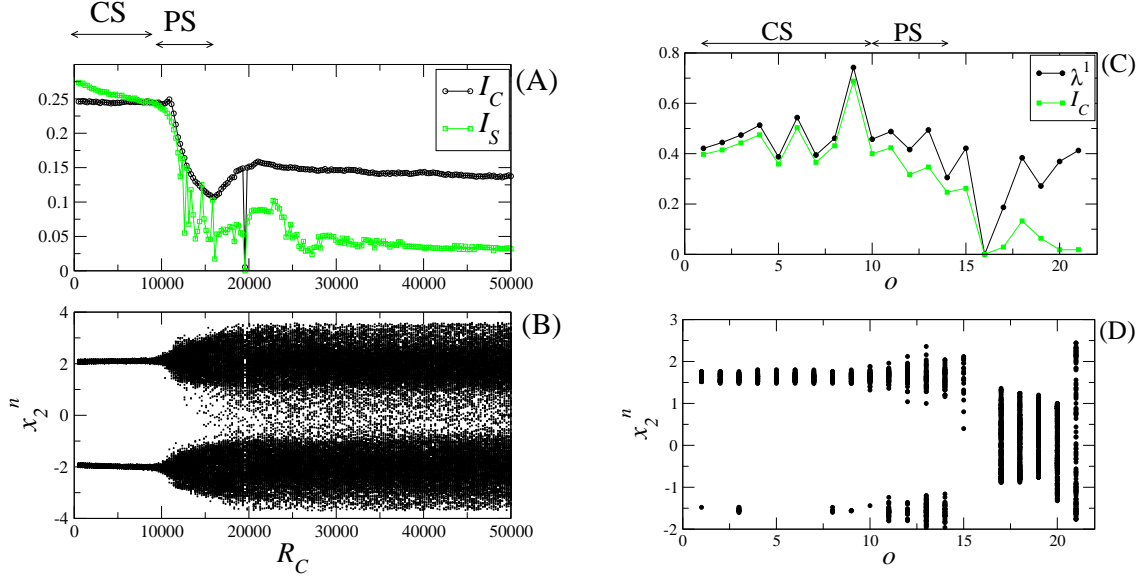


Fig. 3. [Color online] Simulations are shown in (A-B) and experimental results in (C-D). In (A), we show I_C [see Eq. (11)] and I_S [see Eq. (19)]. The Lyapunov exponents of the simulated circuit, with which I_C is calculated, are obtained using the method of Ref. [23] and the variational equations in Eq. (15). Complete synchronization (CS) in the generalized sense [11,12] is observed for $R_C < 9000$ and PS for $9000 \leq R_C \leq 16000$. In (B), we show the conditional observations realized in S_2 at the moment S_1 makes its n -th event, i.e. the crossing of $x_1(\tau)$ with the defined Poincaré sections [conditions (8) and (9)]. A periodic orbit is observed for $R_C \cong 20,000$. In (C), we show λ^1 calculated as described in Sec. 4.1, and I_C is calculated considering that λ^2 is estimated from Eq. (20). CS in the generalized sense is observed for the data series Fo , with $o \leq 10$, and PS for Fo , with $11 \leq o \leq 14$. In (D), we show the conditional observations realized in S_2 at the moment S_1 makes its n -th event, i.e. the crossing of $x_1(t)$ with the defined Poincaré sections [see conditions (5), (6), and (7)]. A periodic orbit is observed for the data set $F16$.

where x_2^n is the value of $x_2(t + \delta)$ at the moment the circuit S_1 makes its n -th event. By an event, we consider conditions (5) and (7). While $[\max(x_2^n) - \min(x_2^n)]$ measures the size of the conditional observations, $[\max(x_2) - \min(x_2)]$ measures the size of the reconstructed attractor.

Thus, if the conditional observations cover the whole attractor, $\lambda^2 = \lambda^1$, and thus $I_C = 0$, which means no information is being transmitted between both circuits, since whenever S_1 crosses the defined Poincaré section, S_2 can be everywhere. If there is complete synchronization in the generalized sense [11,12], $[\max(x_2^n) - \min(x_2^n)] \cong 0$ and $I_C = \lambda^1$, meaning that whenever S_1 crosses the defined Poincaré section, S_2 is also about to or has just crossed that particular section. Therefore, the information about one circuit trajectory by observing the other circuit is maximal.

5 Synchronization versus information

In Figs. 3(A-B), we show results from our numerical simulations, while in Figs. (C-D), experimental results. In both cases, one obvious observation is that the more synchronous the circuits are (small R_C), the larger the rate of information that can be measured in one circuit about the other circuit, being maximal when the two circuits are completely synchronous in the generalized sense [11,12]. When both circuits are in PS, the MIR decreases but remains larger than when there is no PS.

6 Mutual information rate in large active networks

For large active networks with elements arbitrarily connected, an extension of Eq. (10) is

$$I_C(\mathbf{x}_i, \mathbf{x}_j) \leq \max(\lambda) - \lambda^\perp, \quad (21)$$

where $\max(\lambda)$ is the largest Lyapunov exponent of the network and λ^\perp is the transversal exponent between the elements \mathbf{x}_i and \mathbf{x}_j . Making an analogy with the usual definition of mutual information as given by Shannon [22], the term $\max(\lambda)$ provides the rate of information produced by the source, and the term λ^\perp quantifies the error in the transmission. The term $\max(\lambda)$ can be calculated by a scalar signal measured from x_i , and λ^\perp can be estimated either by the ways of Eq. (20) or as similarly done in Ref. [15].

7 Conclusions

This work proposes a rationale to experimentally study the relationship between transmission of information and synchronization in active networks formed by non-identical and non-coherent elements. For the coupled Chua's circuit, we have shown that the larger the level of synchronization the larger the rate of information exchanged between both circuits, which implies that such a system is non-excitable. By non-excitability [9] we mean a system that as the coupling strength increases, the Kolmogorov-Sinai entropy [23] (the sum of the positive Lyapunov exponents) decreases. For such systems, the maximal mutual information rate that can be achieved, the so called channel capacity, happens for when complete (generalized) synchronization is present.

Other relevant contributions of this work include showing that for short time series the largest conditional exponent (demonstrated to be identical to the largest Lyapunov exponent) can only be reliably estimated by using a multivariate data set, with information of both elements being considered, and that the second largest conditional exponent (which also equals the second largest Lyapunov exponent) can only be reliably estimated by the conditional observations, realized in one element when the other makes an event. Finally, we have also shown that for two coupled non-identical and non-coherent systems, phase synchronization can be detected by these conditional observations, even though for such a system phase is not well defined.

8 Appendix

Consider the notation $\mathbf{x} = (\mathbf{x}_1^T, \mathbf{x}_2^T)$ and $\mathbf{X} = (\mathbf{x}_{12}^{\perp T}, \mathbf{x}_{12}^{\parallel T})$, such that

$$\begin{aligned} \dot{\mathbf{x}} &= \mathbf{M}\mathbf{x}, \text{ and} \\ \dot{\mathbf{X}} &= \mathbf{M}_2\mathbf{X} + \mathbf{c}_2, \end{aligned}$$

where

$$\mathbf{M} = \begin{pmatrix} 1 & 0 & 0 & -1 & 0 & 0 \\ 0 & 1 & 0 & 0 & -1 & 0 \\ 0 & 0 & 1 & 0 & 0 & -1 \\ 1 & 0 & 0 & 1 & 0 & 0 \\ 0 & 1 & 0 & 0 & 1 & 0 \\ 0 & 0 & 1 & 0 & 0 & 1 \end{pmatrix} \quad \mathbf{M}_2 = \begin{pmatrix} \frac{\partial \dot{x}_{12}^\perp}{\partial x_{12}^\perp} & \frac{\partial \dot{x}_{12}^\perp}{\partial x_{12}^\parallel} \\ \frac{\partial \dot{x}_{12}^\parallel}{\partial x_{12}^\perp} & \frac{\partial \dot{x}_{12}^\parallel}{\partial x_{12}^\parallel} \end{pmatrix} \quad (22)$$

with the terms in matrix (22) given by

$$\frac{\partial \dot{x}_{12}^\perp}{\partial x_{12}^\perp} = \begin{pmatrix} \left(-\sigma_1 - \frac{\partial g_1(x_{12}^\perp, x_{12}^\parallel)}{\partial x_{12}^\perp} - \sigma_2 \right) & \sigma_1 & 0 \\ \sigma_3 & -\sigma_3 & \sigma_3 \\ 0 & -\sigma_4 & -\sigma_5 \end{pmatrix}, \quad \frac{\partial \dot{x}_{12}^\perp}{\partial x_{12}^\parallel} = \begin{pmatrix} \left(-\sigma_8 - \frac{\partial g_1(x_{12}^\perp, x_{12}^\parallel)}{\partial x_{12}^\parallel} \right) & \sigma_8 & 0 \\ \sigma_7 & -\sigma_7 & \sigma_7 \\ 0 & -\sigma_9 & -\sigma_{10} \end{pmatrix},$$

$$\frac{\partial \dot{x}_{12}^{\parallel}}{\partial x_{12}^{\perp}} = \begin{pmatrix} \left(-\sigma_8 - \frac{\partial g_2(x_{12}^{\perp}, x_{12}^{\parallel})}{\partial x^{\perp}} + \sigma_6 \right) & \sigma_8 & 0 \\ \sigma_7 & -\sigma_7 & \sigma_7 \\ 0 & -\sigma_9 & -\sigma_{10} \end{pmatrix}, \quad \frac{\partial \dot{x}_{12}^{\parallel}}{\partial x_{12}^{\parallel}} = \begin{pmatrix} \left(-\sigma_1 - \frac{\partial g_2(x_{12}^{\perp}, x_{12}^{\parallel})}{\partial x^{\parallel}} \right) & \sigma_1 & 0 \\ \sigma_3 & -\sigma_3 & \sigma_3 \\ 0 & -\sigma_4 & -\sigma_5 \end{pmatrix},$$

where $\sigma_1 = \frac{\alpha_1 + \alpha_2 \tau}{2}$, $\sigma_2 = \left(\frac{\alpha_1 R_1}{R_C} + \frac{\alpha_2 \tau R_8}{R_C} \right)$, $\sigma_3 = \frac{1 + \tau_C}{2}$, $\sigma_4 = \frac{\beta_1 + \beta_2 \tau}{2}$, $\sigma_5 = \frac{\gamma_1 + \gamma_2 \tau}{2}$, $\sigma_6 = \left(\frac{\alpha_2 \tau R_8}{R_C} - \frac{\alpha_1 R_1}{R_C} \right)$, $\sigma_7 = \frac{1 - \tau_C}{2}$, $\sigma_8 = \frac{\alpha_1 - \alpha_2 \tau}{2}$, $\sigma_9 = \frac{\beta_1 - \beta_2 \tau}{2}$, $\sigma_{10} = \frac{\gamma_1 - \gamma_2 \tau}{2}$.

The terms $\frac{\partial g_1(x_{12}^{\perp}, x_{12}^{\parallel})}{\partial x^{\perp}}$, $\frac{\partial g_1(x_{12}^{\perp}, x_{12}^{\parallel})}{\partial x^{\parallel}}$, $\frac{\partial g_2(x_{12}^{\perp}, x_{12}^{\parallel})}{\partial x^{\perp}}$, and $\frac{\partial g_2(x_{12}^{\perp}, x_{12}^{\parallel})}{\partial x^{\parallel}}$ assume different values depending on which of the domains, namely (i), (ii), (iii), (iv), the values of x_1 and x_2 belong to, and are given by

Domains	(i)	(ii)	(iii)	(iv)	
$\frac{\partial g_1(x_{12}^{\perp}, x_{12}^{\parallel})}{\partial x_{12}^{\perp}}$	ξ_8	ξ_5	ξ_1	ξ_4	$\xi_1 = \frac{a_1 \alpha_1 + b_2 \alpha_2 \tau}{2}$
$\frac{\partial g_1(x_{12}^{\perp}, x_{12}^{\parallel})}{\partial x_{12}^{\parallel}}$	ξ_7	ξ_6	ξ_2	ξ_3	$\xi_2 = \frac{a_1 \alpha_1 - b_2 \alpha_2 \tau}{2}$
$\frac{\partial g_2(x_{12}^{\perp}, x_{12}^{\parallel})}{\partial x_{12}^{\perp}}$	ξ_7	ξ_6	ξ_2	ξ_3	$\xi_3 = \frac{a_1 \alpha_1 - a_2 \alpha_2 \tau}{2}$
$\frac{\partial g_2(x_{12}^{\perp}, x_{12}^{\parallel})}{\partial x_{12}^{\parallel}}$	ξ_8	ξ_5	ξ_1	ξ_4	$\xi_4 = \frac{a_1 \alpha_1 + a_2 \alpha_2 \tau}{2}$
					$\xi_5 = \frac{b_1 \alpha_1 + a_2 \alpha_2 \tau}{2}$
					$\xi_6 = \frac{b_1 \alpha_1 - a_2 \alpha_2 \tau}{2}$
					$\xi_7 = \frac{b_1 \alpha_1 - b_2 \alpha_2 \tau}{2}$
					$\xi_8 = \frac{b_1 \alpha_1 + b_2 \alpha_2 \tau}{2}$

where domain (i) is defined by $x_1 \in D_-$ and $x_2 \in D_-$, or $x_1 \in D_-$ and $x_2 \in D_+$; domain (ii) by $x_1 \in D_-$ and $x_2 \in D_0$; domain (iii) by $x_1 \in D_0$ and $x_2 \in D_-$ or $x_2 \in D_+$; and domain (iv) by $x_1 \in D_0$ and $x_2 \in D_0$.

References

1. V. A. Smith, J. Yu, T. V. Smulders, *et al.* PLoS Comput. Biol. **2**, e161 (2006)
2. J. J. Eggermont, Neurosci. Biobehav. Rev. **22**, 355 (1998)
3. A. Borst and F. E. Theunissen, Nature Neurosci. **2**, 947 (1999)
4. S. P. Strong, R. Köberle, R. R. de Ruyter van Steveninck, and W. Bialek, Phys. Rev. Lett. **80**, 197 (1998)
5. M. Palus, V. Komárek, T. Procházka, *et al.* IEEE Eng. Med. Biol. Mag. **Setember/October**, 65 (2001)
6. M. Żochowski and R. Dzakpasu, J. Phys. A **37**, 3823 (2004)
7. T. Schreiber, Phys. Rev. Lett. **85**, 461 (2000)
8. X. San Liang and R. Kleman, Phys. Rev. Lett. **95**, 244101 (2005)
9. M. S. Baptista and J. Kurths, Phys. Rev. E **72**, 045202 (2005); M. S. Baptista and J. Kurths Phys. Rev. E **77**, 026205 (2008); M. S. Baptista, J. X. de Carvalho and M. S. Hussein, PloS ONE **3**, e3479 (2008).
10. L. M. Pecora and T. Carroll, Phys. Rev. Lett. **80**, 2109 (1998)
11. L. M. Pecora, T. Carroll, and J. Heagy, Phys. Rev. E **52**, (1995) 3420-3439; A. Arena, A. Diaz-Guilera, J. Kurths, Y. Moreno, C. Zhou, Phys. Rep. **469**, 93 (2008).
12. Since the circuits present parameter mismatches, the trajectory of one circuit never becomes completely equal to the other circuit. However, one can show [11] that there is a function G , for which it is true that $\mathbf{x}_1 = G(\mathbf{x}_2)$. This type of synchronization is called generalized complete synchronization.
13. S. K. Dana, B. Blasius, and J. Kurths, Chaos **16**, 023111 (2006); P. K. Roy, S. Chakraborty and S. K. Dana, Chaos **13**, 342 (2003).
14. M. S. Baptista, T. Pereira, J. C. Sartorelli, *et al.* Physica D **212**, 216 (2005)
15. T. Pereira, M. S. Baptista, and J. Kurths, Phys. Rev. E **75**, 026216 (2007)
16. A. Pikovsky, M. Rosenblum, and J. Kurths, *Synchronization: A Universal Concept in Nonlinear Sciences* (Cambridge, London 2003).
17. M. S. Baptista, S. Boccaletti, K. Josić, and I. Leyva, Phys. Rev. E **69** 056228 (2004)
18. T. Pereira, M. S. Baptista, and J. Kurths, Phys. Lett. A **362**, 159 (2007)
19. S. P. Garcia, M. Niemann, and H. Kantz, "The spectrum of Lyapunov exponents for the nearest neighbor embedding with different time delays", to be submitted for publication.

20. S. P. Garcia and J.S. Almeida, Phys. Rev. E **71**, 037204 (2005); S.P. Garcia and J.S. Almeida, Phys. Rev. E **72**, 027205 (2005)
21. M.B. Kennel, R. Brown, and H.D.I. Abarbanel, Phys. Rev. A **45**, 3403 (1992)
22. C. E. Shannon and W. Weaver, *The Mathematical Theory of Communication* (The University of Illinois Press, Urbana, Illinois 1949).
23. J.-P. Eckmann and D. Ruelle, Rev. Mod. Phys. **57**, 617 (1985)